Engineering Analysis with Boundary Elements ▮ (▮▮▮▮) ▮▮▮–▮▮▮

Contents lists available at ScienceDirect

Engineering Analysis with Boundary Elements

journal homepage: www.elsevier.com/locate/enganabound

Solution of potential flow problems by the modified method of fundamental solutions: Formulations with the single layer and the double layer fundamental solutions

Božidar Šarler

Laboratory for Multiphase Processes, University of Nova Gorica, Vipavska 13, SI-5000 Nova Gorica, Slovenia

ARTICLE INFO

Article history:
Received 15 March 2009
Accepted 11 June 2009

Keywords:
Potential flow
Method of fundamental solutions
Desingularisation
Two-dimensional Cartesian coordinates
Single layer fundamental solution
Double layer fundamental solution

ABSTRACT

This paper describes an application of the recently proposed modified method of fundamental solutions (MMFS) to potential flow problems. The solution in two-dimensional Cartesian coordinates is represented in terms of the single layer and the double layer fundamental solutions. Collocation is used for the determination of the expansion coefficients. This novel method does not require a fictitious boundary as the conventional method of fundamental solutions (MFS). The source and the collocation points thus coincide on the physical boundary of the system. The desingularised values, consistent with the fundamental solutions used, are deduced from the direct boundary element method (BEM) integral equations by assuming a linear shape of the boundary between the collocation points. The respective values of the derivatives of the fundamental solution in the coordinate directions, as required in potential flow calculations, are calculated indirectly from the considerations of the constant potential field. The normal on the boundary is calculated by parametrisation of its length and the use of the cubic radial basis functions with the second-order polynomial augmentation. The components of the normal are calculated in an analytical way. A numerical example of potential flow around a two-dimensional circular region is presented. The results with the new MMFS are compared with the results of the classical MFS and the analytical solution. It is shown that the MMFS gives better accuracy for the potential, velocity components (partial derivatives of the potential), and absolute value of the velocity as compared with the classical MFS. The results with the single layer fundamental solution are more accurate than the results with the double layer fundamental solution.

1. Introduction

In recent years there has been a strong development of mesh reduction methods in which polygon-like meshes are reduced or avoided. The method of fundamental solutions (MFS) (sometimes also called the F-Trefftz method, charge simulation method, or singularity method) [1–3] is a numerical technique that belongs to the class of methods generally called boundary methods. The other well-known representative of these methods is the boundary element method (BEM) [4,5]. Both methods are best applicable in situations where a fundamental solution of the partial differential equation in question is known. In such cases, the dimensionality of the discretisation is reduced. The BEM, for example, requires polygonisation of the boundary surfaces in general three-dimensional (3D) cases, and boundary curves in general 2D cases. This method requires the solution of complicated regular, weakly singular, strongly singular, and hypersingular integrals over boundary segments which is, usually, a cumbersome and non-trivial task. The MFS [6] has certain advantages over BEM, that stem mostly from the fact only the pointisation of the boundary is needed only, which completely avoids any integral evaluations, and makes no principal difference in coding between the 2D and the 3D cases. On the other hand, when the Laplace operator is involved, the MFS requires, due to the singular fundamental solution, nodes that are positioned on an artificial boundary located outside the computational domain. The location of the artificial boundary represents the most serious problem of the MFS and has to be dealt with heuristically [7]. Both BEM and MFS are ideal candidates for solving a certain class of free and moving boundary problems [8,9]. Some important developments of the MFS, that might be put into connection with the Laplace equation, focused in the present paper, are as follows. The method has been used for harmonic problems with linear [10] and non-linear boundary conditions [11], free boundaries [12,13], multi-domains [14], for heat conduction in isotropic and anisotropic bimaterials [15], and for axisymmetric problems [16]. The method has been expanded for material non-linearities and all technically relevant boundary conditions in a systematic way and applied to thermal design of hollow bricks [17]. The latter paper

E-mail address: bozidar.sarler@p-ng.si

0955-7997/$ - see front matter © 2009 Elsevier Ltd. All rights reserved.
doi:10.1016/j.enganabound.2009.06.008

represents one of the rare industrial applications of the MFS. In the present paper, the potential flow problem, previously solved by the least squares version of MFS [18] and collocation version of MFS [13] is solved by the modified method of fundamental solutions (MMFS). This novel method, which essentially represents a sort of blend between BEM and MFS has been originally developed in [19] by using collocation with the double layer Laplace equation fundamental solution. The method has been further extended to the single layer Laplace equation fundamental solution in [20]. The main drawback of the MFS is to decide the positions of the source points that need to be positioned outside the domain. In case they are too close to the boundary, the solution is not accurate. In case they are too far away from the boundary, the discretisation matrix becomes ill conditioned. The novel MMFS overcomes this difficulty by allowing the source point positions to coincide with the collocation points on the physical boundary. A desingularisation technique thus has to be employed in order to be able to allow bounded values in the discretisation matrix. The desingularisation has been derived through the properties of the double layer potential in [19] and through the indirect BEM formulation [21] in [20]. The MMFS can be seen as a special discrete version of the indirect BEM. In the present paper, the desingularisation technique is put into the context of potential flow problems by using and comparing both, the single layer fundamental solution (SLFS) and the double layer fundamental solution (DLFS). The calculation of the desingularised values of the partial (not normal) derivatives on the boundary is represented as well, which was not the case in the previous two cited MMFS pioneering papers by D.L. Young's group. This paper represents a more complete discussion of the topics, given as an invited lecture at the 30th Boundary Element Methods and Mesh Reduction Techniques Conference in Maribor, Slovenia [22] in 2008.

2. Governing equations

Consider a connected two-dimensional domain Ω with boundary Γ. The domain is filled by a fluid that undergoes potential flow. The boundary is divided into the part Γ^E that represents the external boundaries of the system and into the part Γ^I, that represents internal boundary of the system, i.e. $\Gamma=\Gamma^E\cup\Gamma^I$ (see Fig. 1). The potential Φ is governed by the following boundary value problem: Laplace equation

$$\nabla^2\Phi=0, \tag{1}$$

and boundary conditions of the Dirichlet and Neumann type, located at the Dirichlet Γ^D and Neumann Γ^N parts of the boundary Γ, i.e. $\Gamma=\Gamma^D\cup\Gamma^N$

$$\Phi(\mathbf{p})=\overline{\Phi}^D(\mathbf{p}),\quad \mathbf{p}\in\Gamma^D, \tag{2}$$

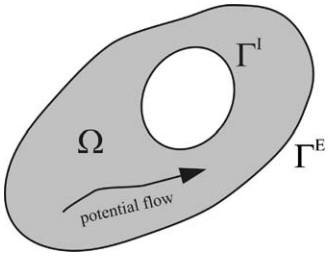

Fig. 1. Problem domain Ω with internal Γ^I and external Γ^E boundaries. Potential flow region is represented in gray.

$$\frac{\partial\Phi}{\partial\mathbf{n}_\Gamma}(\mathbf{p})=\overline{\Phi}^N(\mathbf{p}),\quad \mathbf{p}\in\Gamma^N, \tag{3}$$

with $\mathbf{p}$ denoting the position vector and $\mathbf{n}_\Gamma$ the outward normal on the boundary Γ. $\overline{\Phi}^D$ and $\overline{\Phi}^N$ represent the Dirichlet and Neumann boundary condition forcing functions. Let us introduce a two-dimensional Cartesian coordinate system with ortho-normal base vectors $\mathbf{i}_x$ and $\mathbf{i}_y$ and coordinates p_x and p_y, i.e. $\mathbf{p}=p_x\mathbf{i}_x+p_y\mathbf{i}_y$. The potential field velocity components are calculated from the potential Φ as

$$v_\xi(\mathbf{p})=\frac{\partial\Phi}{\partial p_\xi}(\mathbf{p});\quad \xi=x,y. \tag{4}$$

It is the purpose of this paper to determine the steady-state potential flow components as a function of the posed geometry, governing equation and boundary conditions.

3. Solution procedure

3.1. Solution of the potential flow

The common points of the MFS and MMFS for the solution of the potential flow field are elaborated first. The differences are elaborated afterwards. The solution of the potential Φ is represented by the N_Γ global approximation functions $\psi_n(\mathbf{p})$ and their coefficients α_n

$$\Phi(\mathbf{p})\approx\sum_{n=1}^{N_\Gamma}\psi_n(\mathbf{p})\alpha_n. \tag{5}$$

The global approximation functions have the property

$$\nabla^2\psi_n(\mathbf{p})=\begin{cases}0; & \mathbf{p}\neq\mathbf{p}_n\\ \delta(\mathbf{p}_n); & \mathbf{p}=\mathbf{p}_n\end{cases};\quad n=1,2,\ \ldots,N_\Gamma, \tag{6}$$

that is, they are fundamental solutions of the Laplace operator. δ denotes the Kronecker symbol. For two-dimensional problems in Cartesian coordinates, the single layer fundamental solution is

$$\psi_n^*(\mathbf{p})=\frac{1}{2\pi}\log\frac{r^*}{r_n};\quad r_n^2=\mathbf{r}_n\cdot\mathbf{r}_n,\qquad \mathbf{r}_n=\mathbf{p}-\mathbf{s}_n=(p_x-s_{nx})\mathbf{i}_x+(p_y-s_{ny})\mathbf{i}_y, \tag{7}$$

where r^* denotes the reference radius. The double layer fundamental solution, defined by

$$\psi_n^\diamond(\mathbf{p})=\frac{\partial\psi_n^*}{\partial\mathbf{n}_s}(\mathbf{p})=\frac{1}{2\pi}\left[\frac{(p_x-s_{nx})n_{sx}}{(p_x-s_{nx})^2+(p_y-s_{ny})^2}+\frac{(p_y-s_{ny})n_{sy}}{(p_x-s_{nx})^2+(p_y-s_{ny})^2}\right], \tag{8}$$

is also used in the present paper. $\mathbf{n}_s$ represents the normal to the boundary at the source point $\mathbf{s}$. The following is valid

$$\nabla^2\psi_n^\diamond(\mathbf{p})=\nabla^2\frac{\partial\psi^*}{\partial\mathbf{n}_s}(\mathbf{p})=\frac{\partial}{\partial\mathbf{n}_s}\nabla^2\psi^*(\mathbf{p})=\begin{cases}0; & \mathbf{p}\neq\mathbf{p}_n\\ \dfrac{\partial}{\partial\mathbf{n}_s}\delta(\mathbf{p}_n); & \mathbf{p}=\mathbf{p}_n\end{cases};\quad n=1,2,\ \ldots,N_\Gamma. \tag{9}$$

Let us introduce the boundary condition indicators in order to be able to represent the boundary collocation equations in a compact form. The Dirichlet χ^D and Neumann χ^N type of boundary

Please cite this article as: Šarler B. Solution of potential flow problems by the modified method of fundamental solutions: Formulations with the single layer and the double layer.... Eng Anal Bound Elem (2009), doi:10.1016/j.enganabound.2009.06.008

conditions indicators are

$$\chi^D(\mathbf{p}) = \begin{cases} 1; & \mathbf{p} \in \Gamma^D \\ 0; & \mathbf{p} \notin \Gamma^D \end{cases}, \tag{10}$$

$$\chi^N(\mathbf{p}) = \begin{cases} 1; & \mathbf{p} \in \Gamma^N \\ 0; & \mathbf{p} \notin \Gamma^N \end{cases}. \tag{11}$$

The coefficients are calculated from a system of N_Γ algebraic equations

$$\boldsymbol{\Psi}\boldsymbol{\alpha} = \mathbf{b}; \quad \sum_{n=1}^{N_\Gamma} \Psi_{jn}\alpha_n = b_j; \quad j = 1, 2, \ldots, N_\Gamma, \tag{12}$$

where

$$\Psi_{jn} = \chi^D(\mathbf{p}_j)\psi_n(\mathbf{p}_j) + \chi^N(\mathbf{p}_j)\frac{\partial \psi_n}{\partial \mathbf{n}_\Gamma}(\mathbf{p}_j), \tag{13}$$

$$b_j = \chi^D(\mathbf{p}_j)\overline{\Phi}^D(\mathbf{p}_j) + \chi^N(\mathbf{p}_j)\overline{\Phi}^N(\mathbf{p}_j), \tag{14}$$

and where ψ_n stands either for ψ_n^* or for $\psi_n^\diamond$. The coefficients $\boldsymbol{\alpha}$ can be expressed through inversion of the system (12), which gives

$$\boldsymbol{\alpha} = \overline{\boldsymbol{\Psi}}\mathbf{b}; \quad \alpha_n = \sum_{j=1}^{N_\Gamma} \overline{\Psi}_{nj}[\chi^D(\mathbf{p}_j)\overline{\Phi}^D(\mathbf{p}_j) + \chi^N(\mathbf{p}_j)\overline{\Phi}^N(\mathbf{p}_j)];$$
$$n = 1, 2, \ldots, N_\Gamma, \tag{15}$$

with $\overline{\boldsymbol{\Psi}}$ standing for the inverse of the matrix $\boldsymbol{\Psi}$. The velocity field components are than calculated as

$$v_\xi(\mathbf{p}) = \sum_{n=1}^{N_\Gamma} \frac{\partial \psi_n}{\partial p_\xi}(\mathbf{p})\alpha_n; \quad \xi = x, y. \tag{16}$$

3.2. The classical method of fundamental solutions

The fundamental solution source points are located outside the physical domain, i.e. $\mathbf{p}_j \neq \mathbf{s}_j$ and $\mathbf{s}_j \notin \Omega$ in the classical MFS (see Fig. 2). One can consider that they form an artificial boundary. The proper location of the source points is not a trivial task. It can be observed that the accuracy improves with the increasing of distance from the physical boundary up to some extent. However, the collocation matrices become increasingly ill conditioned with increased distance from the boundary. The explicit forms of the partial derivatives of the introduced fundamental solutions are

$$\frac{\partial \psi^*}{\partial p_\xi}(\mathbf{p}) = -\frac{1}{\pi}\frac{(p_\xi - s_{n\xi})}{(p_x - s_{nx})^2 + (p_y - s_{ny})^2}; \quad \xi = x, y, \tag{17}$$

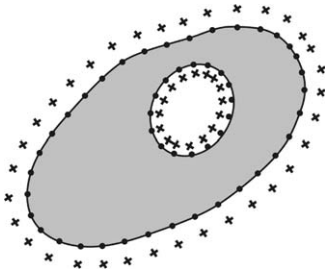

Fig. 2. Discretisation schematics. Symbols • and + represent collocation points and fundamental solution source points, respectively. These points do not coincide in the case of MFS (like in the figure) and coincide in the case of MMFS.

$$\frac{\partial \psi^\diamond}{\partial p_x}(\mathbf{p}) = -\frac{1}{\pi}\frac{(p_x - s_{nx})(p_y - s_{ny})n_{sy}}{[(p_x - s_{nx})^2 + (p_y - s_{ny})^2]^2} + \frac{1}{2\pi}\left[\frac{1}{(p_x - s_{nx})^2 + (p_y - s_{ny})^2} - \frac{2(p_x - s_{nx})(p_x - s_{nx})}{[(p_x - s_{nx})^2 + (p_y - s_{ny})^2]^2}\right] n_{sx}, \tag{18}$$

$$\frac{\partial \psi^\diamond}{\partial p_y}(\mathbf{p}) = -\frac{1}{\pi}\frac{(p_y - s_{ny})(p_x - s_{nx})n_{sy}}{[(p_x - s_{nx})^2 + (p_y - s_{ny})^2]^2} + \frac{1}{2\pi}\left[\frac{1}{(p_x - s_{nx})^2 + (p_y - s_{ny})^2} - \frac{2(p_y - s_{ny})(p_y - s_{ny})}{[(p_x - s_{nx})^2 + (p_y - s_{ny})^2]^2}\right] n_{sy}. \tag{19}$$

3.3. The modified method of fundamental solutions

The key point of the modified method of fundamental solutions lies in the desingularisation of the value of the fundamental solution, in case the source and the collocation points coincide, i.e. $\mathbf{p}_j = \mathbf{s}_j$ (see Fig. 2). The desingularisation value can be directly set from

$$\int_\Gamma \Phi \nabla \psi^* \cdot d\boldsymbol{\Gamma} - \int_\Gamma \psi^* \nabla \Phi \cdot d\boldsymbol{\Gamma} + c(\mathbf{s})\Phi(\mathbf{s}) = 0. \tag{20}$$

The derivation of the upper equation with respect to $\mathbf{n}_s$ gives

$$\int_\Gamma \Phi \nabla \psi^\diamond \cdot d\boldsymbol{\Gamma} - \int_\Gamma \psi^\diamond \nabla \Phi \cdot d\boldsymbol{\Gamma} + c(\mathbf{s})\frac{\partial \Phi}{\partial \mathbf{n}}(\mathbf{s}) = 0. \tag{21}$$

In case of the constant potential Φ, Eq. (20) reduces to

$$\int_\Gamma \Phi \nabla \psi^* \cdot d\boldsymbol{\Gamma} + c(\mathbf{s})\Phi(\mathbf{s}) = -\int_\Gamma \Phi \psi^\diamond d\Gamma + c(\mathbf{s})\Phi(\mathbf{s}) = 0;$$
$$\int_\Gamma \psi^\diamond d\Gamma = c(\mathbf{s}), \tag{22}$$

and Eq. (21) into

$$\int_\Gamma \nabla \psi^\diamond d\boldsymbol{\Gamma} = 0. \tag{23}$$

The calculation of the desingularised value of the SLFS can be directly set as an average value of the fundamental solution over a portion of the boundary. This can be formulated as

$$\psi_j^\diamond(\mathbf{p}_j) = \frac{1}{\ell_{j-}}\int_{\mathbf{p}_{j-1}}^{\mathbf{p}_j} f_j^*[\mathbf{p}(\Gamma)]d\Gamma + \frac{1}{\ell_{j+}}\int_{\mathbf{p}_j}^{\mathbf{p}_{j+1}} f_j^*[\mathbf{p}(\Gamma)]d\Gamma. \tag{24}$$

The average value of the singularity on the boundary can be calculated in closed form [23]

$$\psi_j^*(\mathbf{p}_j) = \frac{1}{4\pi}\left(1 + \log\frac{2r^*}{\ell_{j-}}\right) + \frac{1}{4\pi}\left(1 + \log\frac{2r^*}{\ell_{j+}}\right), \tag{25}$$

where ℓ_j represents the Euclidean distance between the points $\mathbf{p}_{j-1}$ and $\mathbf{p}_j$ on the boundary. The derivatives of the fundamental solution can be calculated in the following indirect way. Let us assume we have a pure Dirichlet problem with all the boundary values set to a constant $\overline{\Phi}^D(\mathbf{p}) = c; \mathbf{p} \in \Gamma$. In this case we obtain

$$\Phi(\mathbf{p}_j) = c = \sum_{n=1}^{N_\Gamma} \psi_n^*(\mathbf{p}_j)\alpha_n^c, \tag{26}$$

Please cite this article as: Šarler B. Solution of potential flow problems by the modified method of fundamental solutions: Formulations with the single layer and the double layer.... Eng Anal Bound Elem (2009), doi:10.1016/j.enganabound.2009.06.008

$$\frac{\partial}{\partial p_\xi}\Phi(\mathbf{p}_j)=0=\sum_{n=1}^{N_\Gamma+3}\frac{\partial}{\partial p_\xi}\psi_n^*(\mathbf{p}_j)\alpha_n^c;\quad \xi=x,y. \tag{27}$$

The desingularised value of the partial derivative can be calculated as

$$\frac{\partial}{\partial p_\xi}\psi_j^*(\mathbf{p}_j)=-\frac{1}{\alpha_j^c}\sum_{\substack{n=1\\ n\neq j}}^{N_\Gamma}\frac{\partial}{\partial p_\xi}\psi_n^*(\mathbf{p}_j)\alpha_n^c;\quad \xi=x,y. \tag{28}$$

The desingularised values of the normal derivatives can be calculated from the desingularised values of the partial derivatives as

$$\frac{\partial}{\partial \mathbf{n}_\Gamma}\psi_j^*(\mathbf{p}_j)=\frac{\partial}{\partial p_x}\psi_j^*(\mathbf{p}_j)n_x(\mathbf{p}_j)+\frac{\partial}{\partial p_y}\psi_j^*(\mathbf{p}_j)n_y(\mathbf{p}_j). \tag{29}$$

The calculation of the desingularised value of the DLFS can be performed through the discretisation of Eq. (23) in the following simple way

$$\sum_{n=1}^{N_\Gamma}\frac{\ell_{n-}+\ell_{n+}}{2}\psi_j^\diamond(\mathbf{p}_n)=c_s(\mathbf{s}_j), \tag{30}$$

$$\psi_j^\diamond(\mathbf{p}_j)=\frac{1}{\ell_{j-}+\ell_{j+}}\left[1-\sum_{\substack{n=1\\ n\neq j}}^{N_\Gamma}(\ell_{n-}+\ell_{n+})\psi_j^\diamond(\mathbf{p}_n)\right], \tag{31}$$

where we set $c_s(\mathbf{s}_j)=1/2$ in Eq. (30), since it assumed the boundary is smooth. The calculation of the desingularised value of the DLFS normal derivatives can be performed through discretisation of Eq. (23) in the following simple way

$$\sum_{n=1}^{N_\Gamma}\frac{\ell_{n-}+\ell_{n+}}{2}\frac{\partial\psi_n^\diamond}{\partial\mathbf{n}_\Gamma}(\mathbf{p}_j)=0, \tag{32}$$

$$\frac{\partial\psi_j^\diamond}{\partial\mathbf{n}_\Gamma}(\mathbf{p}_j)=-\frac{1}{\ell_{j-}+\ell_{j+}}\left[\sum_{\substack{n=1\\ n\neq j}}^{N_\Gamma}(\ell_{n-}+\ell_{n+})\frac{\partial\psi_j^\diamond}{\partial\mathbf{n}_\Gamma}(\mathbf{p}_j)\right]. \tag{33}$$

The calculation of the derivatives of the potentials in the x- and y-directions at singular points is performed through the derivation of Eq. (31)

$$\frac{\partial}{\partial p_\xi}\psi_j^\diamond(\mathbf{p}_j)=-\frac{1}{\ell_{j-}+\ell_{j+}}\left[\sum_{\substack{n=1\\ n\neq j}}^{N_\Gamma}(\ell_{n-}+\ell_{n+})\frac{\partial}{\partial p_\xi}\psi_j^\diamond(\mathbf{p}_n)\right];\quad \xi=x,y. \tag{34}$$

The desingularised values of $\partial\psi_j{}^\diamond/\partial p_x$, $\partial\psi_j{}^\diamond/\partial p_y$, and $\partial\psi_j{}^\diamond/\partial\mathbf{n}_\Gamma$ can be alternatively calculated from Eqs. (26)–(29) by replacing $\psi_j{}^\diamond$ by $\psi_j{}^*$. This is also the case in the represented numerical examples of the present paper. The internal and external boundaries are given by a vector of points $\mathbf{p}_k$; $k=1,2,\ldots,N_\Gamma{}^B$; $B=I,E$. The length ℓ_k of the contour between the boundary points $\mathbf{p}_k$ and $\mathbf{p}_{k\pm1}$ is parametrised by the simple Euclidean distance

$$\ell_{k\pm}=[(p_{kx}-p_{k\pm1x})^2+(p_{ky}-p_{k\pm1y})^2]^{1/2}, \tag{35}$$

with the cyclic index conditions $k-1=N_\Gamma{}^B$; $k=1$, $k+1=1$; $k=N_\Gamma{}^B$. The total Euclidean length ℓ_Γ of the boundary contour equals

$$\ell_\Gamma=\sum_{k=1}^{N_\Gamma^I}\ell_k^I+\sum_{k=1}^{N_\Gamma^E}\ell_k^E, \tag{36}$$

with $\ell_k{}^I$ and $\ell_k{}^E$ standing for the boundary contour segments of the internal and external boundaries.

3.4. Calculation of the normal on the boundary

The position of the boundary contour between the boundary points can be estimated by the meshless approximation with the contour parameter ℓ

$$p_\xi(\ell)=\sum_{k=1}^{N_\Gamma^B+3}\psi_k(\ell)\alpha_k^\xi;\quad \xi=x,y. \tag{37}$$

The cubic splines

$$\psi_k(\ell)=|\ell-\ell_k|^3;\quad k=1,2,\ldots,N_\Gamma^B, \tag{38}$$

with the augmented functions

$$\psi_{N_\Gamma^B+1}(\ell)=1, \tag{39}$$

$$\psi_{N_\Gamma^B+2}(\ell)=\ell, \tag{40}$$

$$\psi_{N_\Gamma^B+3}(\ell)=\ell^2, \tag{41}$$

are used for the global approximation. The following three compatibility conditions are needed

$$\sum_{k=1}^{N_\Gamma^B+3}\psi_k(0)\alpha_k^\xi=\sum_{k=1}^{N_\Gamma^B+3}\psi_k(\ell_\Gamma)\alpha_k^\xi;\quad \xi=x,y, \tag{42}$$

$$\sum_{k=1}^{N_\Gamma^B+3}\frac{d}{d\ell}\psi_k(0)\alpha_k^\xi=\sum_{k=1}^{N_\Gamma^B+3}\frac{d}{d\ell}\psi_k(\ell_\Gamma)\alpha_k^\xi;\quad \xi=x,y, \tag{43}$$

$$\sum_{k=1}^{N_\Gamma^B+3}\frac{d^2}{d\ell^2}\psi_k(0)\alpha_k^\xi=\sum_{k=1}^{N_\Gamma^B+3}\frac{d^2}{d\ell^2}\psi_k(\ell_\Gamma)\alpha_k^\xi;\quad \xi=x,y, \tag{44}$$

in order to ensure the continuity and the smoothness of the first and the second derivatives required in the calculation of the normal. The coefficients are calculated from a system of $N_\Gamma{}^B$+3 algebraic equations

$$\sum_{k=1}^{N_\Gamma^B+3}\Psi_{kn}\alpha_n^\xi=b_k^\xi;\quad n=1,2,\ldots,N_\Gamma^B+3,\quad \xi=x,y. \tag{45}$$

Table 1
RMS error of the solution as a function of the number of collocation points on the circle boundary. MMFS based on SLFS.

N^I	Φ_{rms}	$v_{x\mathrm{rms}}$	$v_{y\mathrm{rms}}$
64	4.3769614E−04	0.0053239	0.0091937
128	4.4850865E−05	0.0052270	0.0090230
256	4.4021808E−05	0.0051796	0.0089396

Table 2
RMS error of the solution as a function of the number of collocation points on the circle boundary. MMFS based on DLFS.

N^I	Φ_{rms}	$v_{x\mathrm{rms}}$	$v_{y\mathrm{rms}}$
64	5.225166E−04	0.0060698	0.0104648
128	4.806703E−05	0.0060203	0.0103831
256	4.524209E−05	0.0059957	0.0103427

Please cite this article as: Šarler B. Solution of potential flow problems by the modified method of fundamental solutions: Formulations with the single layer and the double layer.... Eng Anal Bound Elem (2009), doi:10.1016/j.enganabound.2009.06.008

The first $N_\Gamma{}^B$ equations are obtained through collocation of Eq. (37) for x- and y-directions at the collocation points ℓ_k; $k = 1, 2, \ldots, N_\Gamma{}^B$ for $n = 1, 2, \ldots, N_\Gamma{}^B+3$, distributed over Γ^B, with

$$\Psi^{\xi}_{kn} = \psi_n(\ell_k); \quad \xi = x, y, \tag{46}$$

Table 3
Error of the solution in terms of v_{rms} as a function of the solution procedure.

$N_\Gamma{}^I$	MFS-SLFS	MFS-DLFS	MMFS-SLFS	MMFS-DLFS
64	0.0150628	0.0150657	0.0132799	0.0151222
128	0.0106511	0.0106617	0.0092168	0.0106085
256	0.0075315	0.0075542	0.0064574	0.0074718

$$b^{\xi}_k = p_{k\xi}; \quad \xi = x, y. \tag{47}$$

The remaining three equations are obtained through the compatibility conditions

$$\Psi^{\xi}_{(N_\Gamma^B+1)n} = \psi_n(\ell_\Gamma) - \psi_n(0); \quad \xi = x, y, \tag{48}$$

$$b^{\xi}_k = 0; \quad k = N_\Gamma^B + 1, \ \xi = x, y, \tag{49}$$

$$\Psi^{\xi}_{(N_\Gamma^B+2)n} = \frac{d\psi_k}{d\ell}(\ell_\Gamma) - \frac{d\psi_k}{d\ell}(0); \quad \xi = x, y, \tag{50}$$

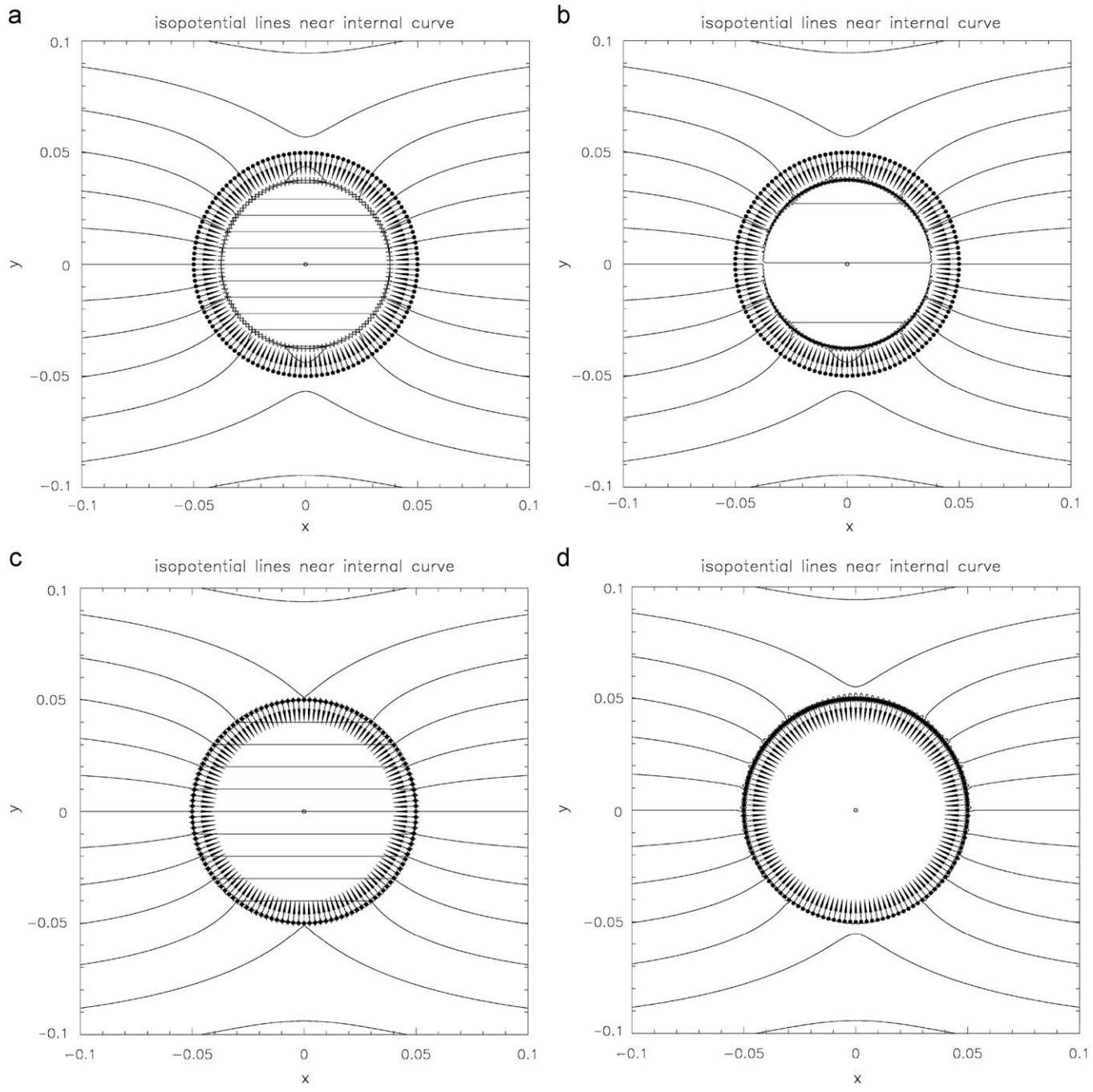

Fig. 3. (a) Potential around circle. MFS with SLFS. The difference between the isopotential lines is 0.02 m^2/s. Note the presence of the internal fictitious boundary. (b) Potential around circle. MFS with DLFS. Note the presence of the internal fictitious boundary. (c) Potential around circle. MMFS with SLFS. Note the coincidence of the source and the collocation points. (d) Potential around circle. MMFS with DLFS. Note the coincidence of the source and the collocation points.

Please cite this article as: Šarler B. Solution of potential flow problems by the modified method of fundamental solutions: Formulations with the single layer and the double layer.... Eng Anal Bound Elem (2009), doi:10.1016/j.enganabound.2009.06.008

$$b_k^{\xi} = 0; \quad k = N_\Gamma^B + 2, \ \xi = x, y, \tag{51}$$

$$\Psi^{\xi}_{(N_\Gamma^B+3)n} = \frac{d^2\psi_n}{d\ell^2}(\ell_\Gamma) - \frac{d^2\psi_n}{d\ell^2}(0); \quad \xi = x, y, \tag{52}$$

$$b_k^{\xi} = 0; \quad k = N_\Gamma^B + 3. \tag{53}$$

The coefficients ${\alpha_n}^x$ and ${\alpha_n}^y$ can be expressed through inversion of the related two systems (37)

$$\alpha_n^{\xi} = \sum_{k=1}^{N_\Gamma^B} \Psi^{\xi-1}_{nk} p_k^{\xi}; \quad \xi = x, y. \tag{54}$$

The components of the normal on the boundary can be explicitly calculated as

$$n_{\Gamma x} = +\frac{dp_y}{d\ell}\left[\left(\frac{dp_x}{d\ell}\right)^2 + \left(\frac{dp_y}{d\ell}\right)^2\right]^{-1/2}, \tag{55}$$

$$n_{\Gamma y} = -\frac{dp_x}{d\ell}\left[\left(\frac{dp_x}{d\ell}\right)^2 + \left(\frac{dp_y}{d\ell}\right)^2\right]^{-1/2}. \tag{56}$$

4. Numerical example

Potential flow around a circle is considered for a numerical example. The flow is confined to a square (exterior) region Γ^E, ${p_x}^- \le p_x \le {p_x}^+$, ${p_y}^- \le p_y \le {p_y}^+$ with ${p_x}^+ = -{p_x}^- = p_0$, ${p_y}^+ = -{p_y}^- = p_0$. The Dirichlet boundary conditions are defined on the square boundaries as

$$\overline{\Phi}^D(p_x, p_y) = v_0 p_y; \quad p_x = p_x^{\pm}, p_y = p_y^{\pm}. \tag{57}$$

The potential field, defined from the boundary conditions (57) gives the following solution for the velocity field

$$v_{0x} = 0, \tag{58}$$

$$v_{0y} = v_0. \tag{59}$$

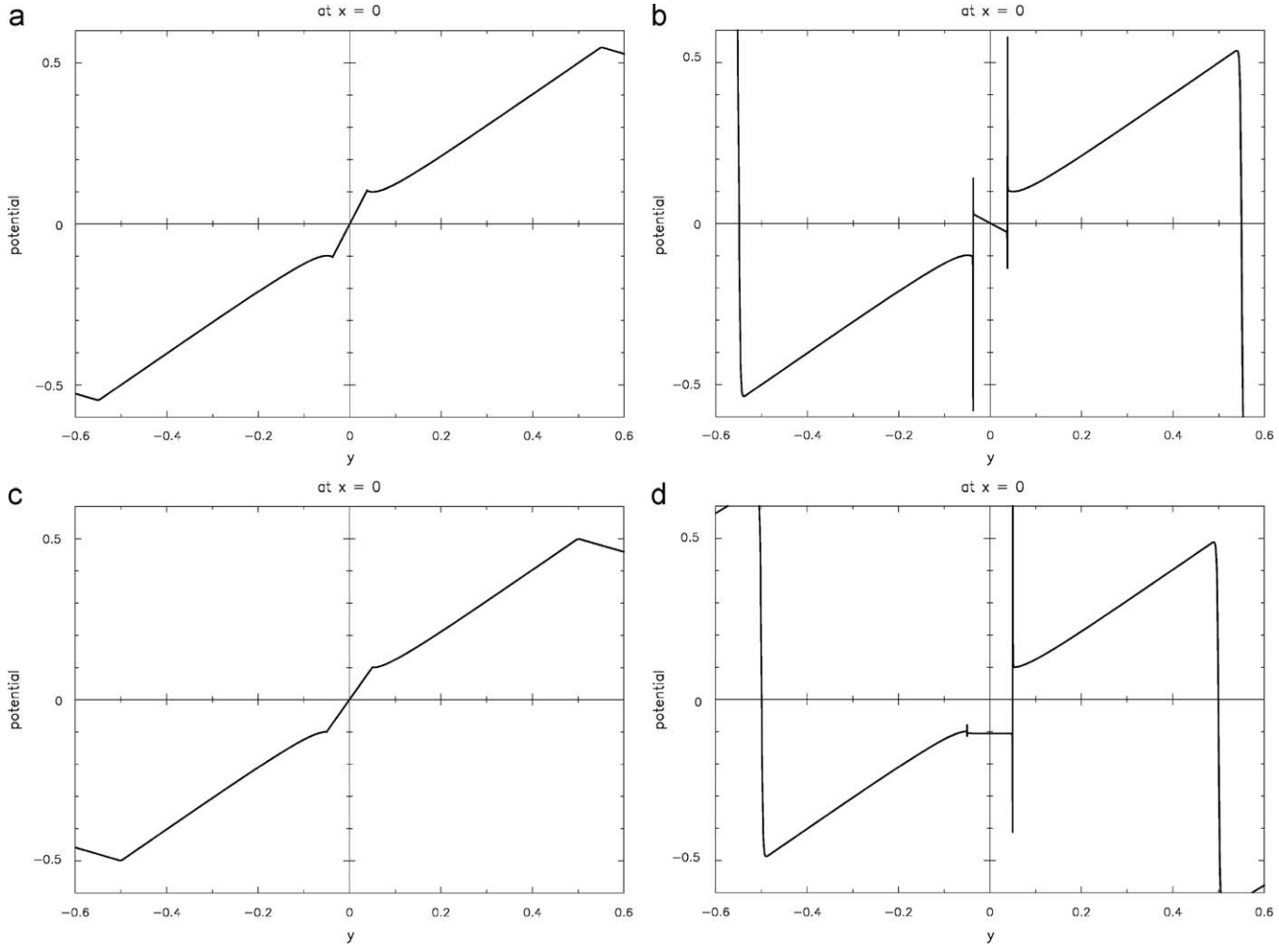

Fig. 4. (a) Calculated potential as a function of the square height at the square centerline. MFS with SLFS. The jumps in derivatives coincide with the artificial boundary positions. (b) Calculated potential as a function of the square height at the square centerline. MFS with DLFS. The jumps in the derivatives coincide with the artificial boundary positions. (c) Calculated potential as a function of the square height at the square centerline. MMFS with SLFS. The jumps in the derivatives coincide with the physical boundary. (d) Calculated potential as a function of the square height at the square centerline. MMFS with DLFS. The jumps in the derivatives coincide with the physical boundary.

Please cite this article as: Šarler B. Solution of potential flow problems by the modified method of fundamental solutions: Formulations with the single layer and the double layer.... Eng Anal Bound Elem (2009), doi:10.1016/j.enganabound.2009.06.008

A circular hole Γ^I (internal boundary) with radius r_0, centered at the point $\mathbf{p}_c$ with coordinates $p_{cx}=(p_x^+ + p_x^-)/2$, $p_{cy}=(p_y^+ + p_y^-)/2$ with Neumann boundary conditions

$$\overline{\Phi}^N[p_x(\Gamma^I), p_y(\Gamma^I)] = 0; \quad \mathbf{p} \in \Gamma^I, \tag{60}$$

is inserted into the square. The solution of the potential field for $r_0 \ll p_0$ equals to

$$\Phi = v_{0y}(p_y - p_{cy})\left[1 + \frac{r_0^2}{(p_x - p_{cx})^2 + (p_y - p_{cy})^2}\right], \tag{61}$$

with v_{0y} defined from Eq. (43). The respective analytical solution for the velocity field is

$$v_x = -v_{0x}\frac{2v_{0y}r_0^2(p_x - p_{cx})(p_y - p_{cy})}{(p_x - p_{cx})^2 + (p_y - p_{cy})^2}, \tag{62}$$

$$v_{\text{ana } y} = v_{0x}\left[1 + \frac{r_0^2}{(p_x - p_{cx})^2 + (p_y - p_{cy})^2}\right] - \frac{2v_{0y}r_0^2(p_y - p_{cy})^2}{(p_x - p_{cx})^2 + (p_y - p_{cy})^2}. \tag{63}$$

We set $r_0 = 0.05$ m, $p_0 = 0.5$ m for defining the geometry. The square sides are virtually divided into 50 equal length segments and the collocation points are placed at each of the segment centers. The total number of discretisation points on the external boundary is set to $N^E = 200$. The presented results are not sensitive to further increase of the number of exterior boundary nodes. In case of the MFS, the source points are moved for 5 nodal distances in the direction of the outward normal on the external boundary. In case this distance was more than 10, the results became unsymmetric, indicating the ill conditioning of the matrix. In the case of the internal boundary, the source point boundaries are put on the artificial boundary with radius $r_{0s} < r_0$. The distances between the source points on this boundary and the distances between the source points and the corresponding collocation points are forced to be the same, i.e.

$$r_0 - r_{0s} = 2\pi r_{0s}/N^I. \tag{64}$$

From this equation, the radius of the circle on which the source points are distributed, is calculated as

$$r_{0s} = \frac{r_0}{1 + (2\pi/N^I)}. \tag{65}$$

In the MMFS, the source points are coincident with the boundary points. The root mean square (RMS) error of the

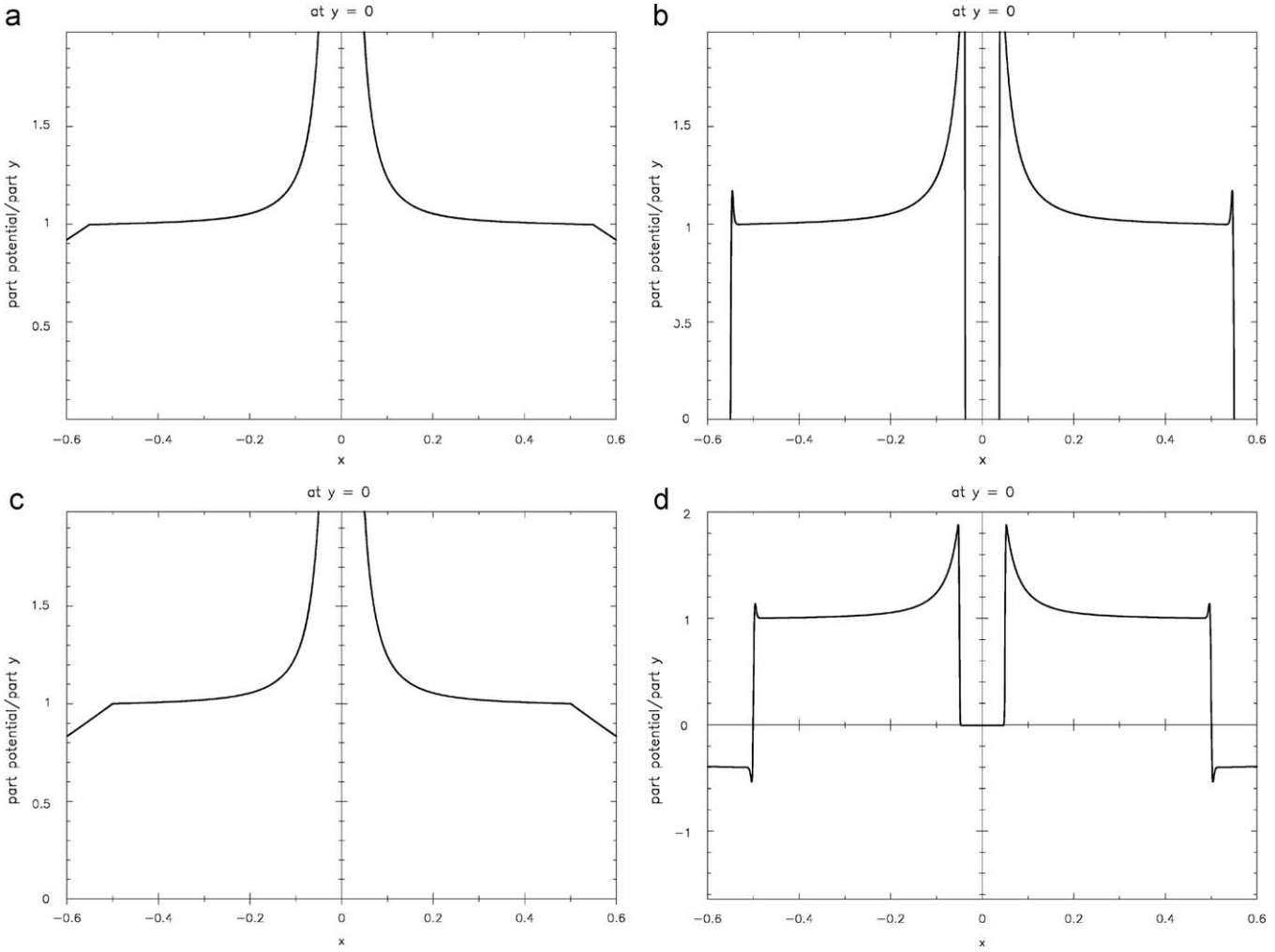

Fig. 5. (a) Calculated potential as a function of the square width at the square centerline. MFS with SLFS. (b) Calculated potential as a function of the square width at the square centerline. MFS with DLFS. (c) Calculated potential as a function of the square width at the square centerline. MMFS with SLFS. (d) Calculated potential as a function of the square width at the square centerline. MMFS with DLFS.

Please cite this article as: Šarler B. Solution of potential flow problems by the modified method of fundamental solutions: Formulations with the single layer and the double layer.... Eng Anal Bound Elem (2009), doi:10.1016/j.enganabound.2009.06.008

numerical solution is defined as

$$\Phi_{\mathrm{rms}} = \sum_{n=1}^{NI} \left\{ \frac{1}{N^I} [\Phi(\mathbf{p}_n) - \Phi_{\mathrm{ana}}(\mathbf{p}_n)]^2 \right\}^{1/2}, \tag{66}$$

$$v_{\xi\,\mathrm{rms}} = \sum_{n=1}^{N^I} \left\{ \frac{1}{N^I} [v_\xi(\mathbf{p}_n) - v_{\xi\,\mathrm{ana}}(\mathbf{p}_n)]^2 \right\}^{1/2}; \quad \xi = x, y, \tag{67}$$

$$v_{\mathrm{rms}} = (v_{x\,\mathrm{rms}}^2 + v_{y\,\mathrm{rms}}^2)^{1/2}. \tag{68}$$

The RMS errors of the potential and velocity components as a function of the discretisation density N^I are, in the case of the MMFS with SLFS, given in Table 1, and with DLFS in Table 2. One can observe monotone convergence of the results with finer discretisation. The results of the MMFS with SLFS are slightly better than the results of the MMFS with DLFS. A comparison of respective errors of the absolute velocity for the MFS and the MMFS with two different types of fundamental solutions weighting is represented in Table 3. One can observe almost the same results when using the MFS with SLFS and DLFS. The potential, velocity components, and absolute value of velocity are better predicted by the present MMFS than in the classical MFS in all attempted discretisations. Among the two MMFS variants, the results with SLFS are better than the results with the DLFS. The preferable choice among the four variants is thus the MMFS-SLFS. Fig. 3 represents the potential field of the four solution procedures used. Fig. 4 represents the calculated potential as a function of the square height at the square centerline as a function of the four variants. Fig. 5 represents the calculated potential as a function of the square width at the square centerline. Figs. 6–9 represent the calculated potential, velocity components, and absolute velocity as a function of the inner boundary position. The most accurate solution (MMFS with SLFS) is for $N_\Gamma = 128$ plotted in Figs. 6–9.

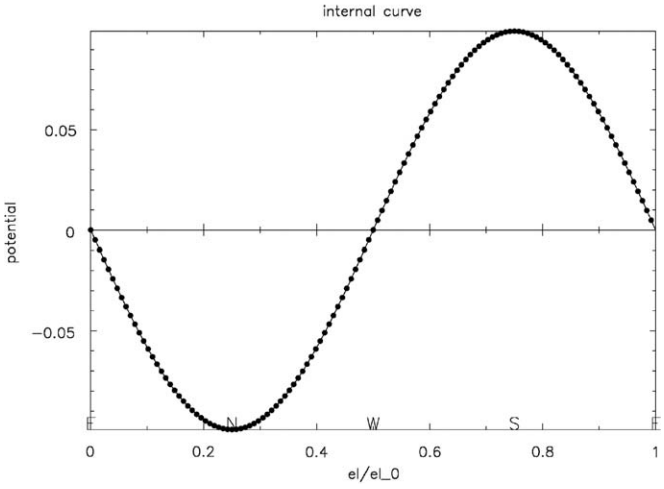

Fig. 6. Calculated potential on the circle. MMFS with SLFS.

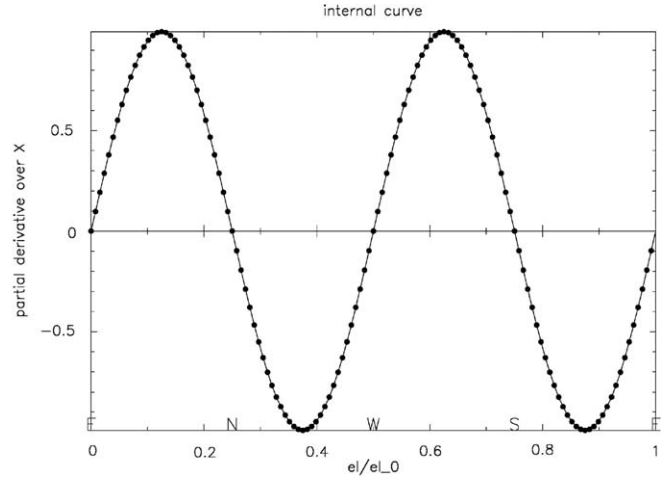

Fig. 7. Calculated x component of the velocity on the circle. MMFS with SLFS.

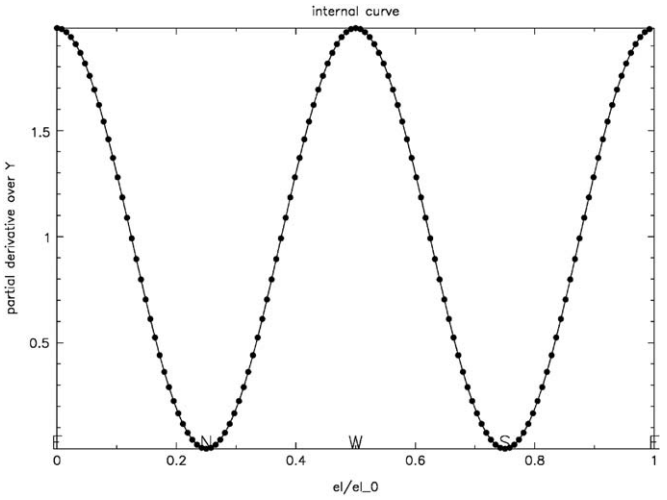

Fig. 8. Calculated y component of the velocity on the circle. MMFS with SLFS.

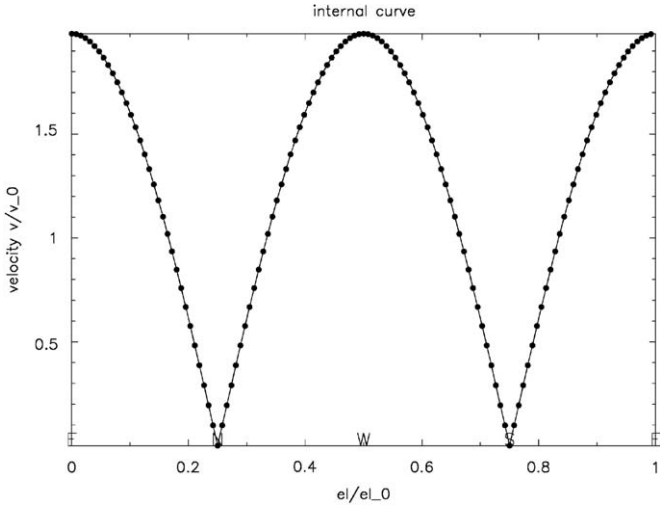

Fig. 9. Calculated absolute value of the velocity on the circle. MMFS with SLFS.

5. Conclusions

In recent years, the MFS has proved to be an effective alternative to the boundary element method for certain problems. Due to its advantages with respect to the simplicity of formulation and the fact that the distribution of the calculation nodes is truly meshless, the method is an ideal candidate for also solving moving and free boundary problems. Its main drawback is the "artificial boundary issue". This issue has been overcome in this work through the MMFS concept, first developed in [19,20]. In this paper, their concept has been used with the SLFS and the DLFS for the first time for potential flow problems, where the accurate representation of the derivatives in addition to the potential on

Please cite this article as: Šarler B. Solution of potential flow problems by the modified method of fundamental solutions: Formulations with the single layer and the double layer.... Eng Anal Bound Elem (2009), doi:10.1016/j.enganabound.2009.06.008

the boundary plays an important role. The desingularisation of the potential has been in the present work made through direct BEM integral equations and the assumption of a straight line boundary geometry between the boundary points. The desingularisation of the spatial derivatives has been made in an indirect way through the constant potential field concept. Only the discretisation nodes on the real boundary are thus required. Both approaches differ from the previous two pioneering works on the subject [19,20]. In addition, this paper extends the MMFS to potential flow situations. The potential and the components of the flow field are calculated more accurately with the MMFS than with the MFS in all discretisations used. The represented developments can be straightforwardly upgraded to axisymmetric problems [16] by the inclusion of the axisymmetric fundamental solution. The flow physics can be extended to Navier–Stokes flow by the strategy, proposed in [24] which uses the dual reciprocity with radial basis functions. The axisymmetric radial basis functions, such as thin plate splines [25] and multiquadrics [26] can be used for this purpose in axisymmetric problems.

Acknowledgement

The author cordially thanks late Professor Michael Golberg for inspiring and unforgettable scientific, philosophical, and gastronomical discussions as well as for very kindly hosting him several times at his home in Las Vegas.

References

[1] Golberg MA, Chen CS. Discrete projection methods for integral equations. Southampton: Computational Mechanics Pubications; 1997.
[2] Golberg MA, Chen CS. The method of fundamental solutions for potential, Helmholtz and diffusion problems. In: Golberg MA, editor. Boundary integral methods—numerical and mathematical aspects. Southampton: Computational Mechanics Publications; 1998. p. 103–76.
[3] Chen CS, Karageorghis A, Smyrlis YS, editors. The method of fundamental solutions—a meshless method. Atlanta: Dynamic Publishers; 2008.
[4] Wrobel LC. The boundary element method, volume I: applications in termo-fluids and acoustics. London: Willey; 2002.
[5] Aliabadi MH. The boundary element method, volume II: applications in solids and structures. London: Willey; 2002.
[6] Fairweather G, Karageorghis A. The method of fundamental solutions for elliptic boundary value problems. Advances in Computational Mathematics 1998;9:69–95.
[7] Balakrishnan K, Ramachadran PA. The method of fundamental solutions for linear diffusion-reaction equations. Mathematical and Computer Modelling 2000;31:221–37.
[8] Hou TY, Lowengrub JS, Shelley MJ. Boundary integral methods for multi-component fluids and multiphase materials. Journal of Computational Physics 2001;169:302–26.
[9] Johnston RL, Fairweather G. The method of fundamental solutions for problems in potential flow. Applied Mathematical Modelling 1984;8:265–70.
[10] Fenner RT. Source field superposition analysis of two dimensional potential problems. International Journal of Numerical Methods in Engineering 1991; 32:1079–91.
[11] Karageorghis A, Fairweather G. The method of fundamental solutions for the solution of nonlinear plane potential problems. IMA Journal of Numerical Analysis 1989;9:231–42.
[12] Karageorghis A. The method of fundamental solutions for the solution of steady state free boundary problems. Journal of Computational Physics 1992;98:119–28.
[13] Šarler B. Solution of a two-dimensional bubble shape in potential flow by the method of fundamental solutions. Engineering Analysis with Boundary Elements 2006;30:227–35.
[14] Leitao VMA. On the implementation of a multi-region Trefftz-collocation formulation for 2-D potential problems. Engineering Analysis with Boundary Elements 1997;20:51–61.
[15] Berger JR, Karageorghis A. The method of fundamental solutions for heat conduction in layered materials. International Journal for Numerical Methods in Engineering 1999;45:1618–94.
[16] Karageorghis A, Fairweather G. The method of fundamental solutions for axisymmetric potential problems. International Journal of Numerical Methods in Engineering 1999;44:1653–69.
[17] Šarler B, Vertnik R, Savić M, Chen CS. A meshless approach to hollow-brick temperature field. In: Atluri SN, Pepper DW, editors. Advances in computational engineering & sciences. Encinio: Tech Science Press; 2002. p. 6.
[18] Johnston RL, Fairweather G. The method of fundamental solutions for problems in potential flow. Applied Mathematical Modelling 1984;8:265–70.
[19] Young DL, Chen KH, Lee CW. Novel meshless method for solving the potential problems with arbitrary domain. Journal of Computational Physics 2005;209: 290–322.
[20] Young DL, Chen JT, Kao JH. A modified method of fundamental solutions with source on the boundary for solving Laplace equations with circular and arbitrary domains. CMES: Computer Modelling in Engineering and Sciences 2007;19:197–221.
[21] Banerjee PK, Butterfield R. Boundary element methods in engineering. New York: McGraw Hill; 1981.
[22] Šarler B. Desingularised method of double layer fundamental solutions for potential flow problems. In: Škerget L, Brebbia CA, editors. Boundary elements and other mesh reduction methods XXX. Southampton & Boston: WIT Press; 2008. p. 159–68.
[23] Rek Z, Šarler B. Analytical integration of elliptic 2D fundamental solution and its derivatives for straight-line elements with constant interpolation. Engineering Analysis with Boundary Elements 1999;5–6:515–25.
[24] Šarler B. Towards a mesh-free solution of transport phenomena. Engineering Analysis with Boundary Elements 2002;26:731–8.
[25] Šarler B. Axisymmetric augmented thin plate splines. Engineering Analysis with Boundary Elements 1998;21:81–5.
[26] Šarler B, Jelić N, Kovačević I, Lakner M, Perko J. Axisymmetric multiquadrics. Engineering Analysis with Boundary Elements 2006;30:137–42.

Please cite this article as: Šarler B. Solution of potential flow problems by the modified method of fundamental solutions: Formulations with the single layer and the double layer.... Eng Anal Bound Elem (2009), doi:10.1016/j.enganabound.2009.06.008